# Uptake of Carbon-11-Methionine and Fluorodeoxyglucose in Non-Hodgkin's Lymphoma: A PET Study

Sirkku Leskinen-Kallio, Ulla Ruotsalainen, Kjell Någren, Mika Teräs, and Heikki Joensuu

*Department of Oncology and Radiotherapy and Turku Medical Cyclotron-PET Center, Turku University Central Hospital, Turku, Finland, and Medical Cyclotron Laboratory, University of Turku, Turku, Finland*

Uptake of L-[methyl-$^{11}$C]methionine ($^{11}$C-methionine) and [$^{18}$F]-2-fluoro-2-deoxy-D-glucose (FDG) was studied with PET in 14 patients with non-Hodgkin's lymphomas. The low molecular weight fraction of venous plasma separated by fast gel filtration was used as the input function for $^{11}$C-methionine studies, and tracer accumulation was analyzed according to Patlak and Gjedde. The average uptake rate of $^{11}$C-methionine was 0.0775 ± 0.0245 min$^{-1}$ (s.d.) and of FDG 0.0355 ± 0.0293 min$^{-1}$, $^{11}$C-methionine uptake rate being significantly higher than that of FDG ($p < 0.01$). Carbon-11-methionine accumulated strongly in all but one of the lymphomas. FDG accumulated clearly in lymphomas of high-grade malignancy, whereas two intermediate- and three low-grade malignant lymphomas had a poor uptake rate. The tumor/plasma ratio of both $^{11}$C-methionine and FDG increased faster in high and intermediate-grade lymphomas than in low-grade lymphomas, but there was considerable overlap between the histologic grades. Carbon-11-methionine seems to be preferable in detecting tumors, while FDG was superior to $^{11}$C-methionine in distinguishing the high-grade malignant lymphomas from the other grades.

**J Nucl Med 1991; 32:1211–1218**

The positron-emitting radiopharmaceutical [$^{18}$F]-2-fluoro-2-deoxy-D-glucose (FDG) has been successfully used in studies on glucose metabolism in vivo (*1*). Phosphorylation by hexokinase of 2-deoxy-D-glucose, an analog of D-glucose, produces 2-deoxy-D-glucose 6-phosphate, which is a relatively poor substrate for the subsequent metabolic steps and is considered to be metabolically trapped intracellularly (*2,3*). In neoplastic tissues, the activity of glucose 6-phosphatase is low (*1,4*). The rate at which FDG accumulates in tumor tissue thus depends essentially on the tracer transport and hexokinase activity of the cells.

Methionine metabolism is also altered in cancer (*5*). Methionine is needed for protein synthesis and for conversion to S-adenosylmethionine, which is the predominant biologic methyl group donor, and a precursor in polyamine synthesis and transsulfuration pathway. Cancer cells are dependent on the external supply of methionine (*5–7*), and the transmethylation rate is high in tumor cells (*8*). The difference in the rates of uptake of amino acids between transformed and nontransformed cells may be 2.5–3.5-fold (*9*).

The aim of this investigation was to study the uptake of L-[methyl-$^{11}$C]methionine ($^{11}$C-methionine) and FDG in non-Hodgkin's lymphoma (NHL), and to study the correlation between histology, proliferative activity, and kinetics and accumulation of $^{11}$C-methionine and FDG in NHL.

## MATERIALS AND METHODS

### Patients

Patients admitted consecutively to Turku University Central Hospital with the diagnosis of lymphoma who were willing to undergo PET imaging were studied. Four patients had high-grade lymphoma, five intermediate-grade, and five low-grade lymphoma (Table 1). Patient 11 had maturity onset-type diabetes, while the remaining patients had normal blood sugar levels. Histology was classified according to the Working Formulation (*10*).

There was no therapy given to those patients with primary lymphoma prior to the PET study. The patients who relapsed had been without any therapy for at least 1 yr, except Patients 6, 7, 8, and 10. Patients 6 and 7 received radiotherapy and the last fraction was given 1.5 mo before the PET study. The lymphoma tumors were large in both cases and they increased in size after radiotherapy. These two patients died of their lymphoma a few months after the PET study. Patient 8 received the last prednisolone dose 1 mo and the last chlorambucile dose 1.5 mo before the PET study. Patient 8 had a low-grade tumor whose size had not changed during the therapy but started to grow after cessation of the treatment. Patient 10 received three doses of chemotherapy with a combination of cyclophosphamide, vincristine, doxorubicin, and prednisolone. There was a 1-mo period after the last therapy and the tumor continued to grow all the time despite the therapy. This patient died 1 mo after the PET study.

The fraction of cells in the S-phase was determined by DNA

Received Jul. 10, 1990; revision accepted Dec. 17, 1990.
For reprints contact: Sirkku Leskinen-Kallio, MD, Department of Oncology and Radiotherapy, Turku University Central Hospital, 20520 Turku, Finland.

**TABLE 1**
Patient Characteristics

| Patient no. | Age/Sex | Lesion size (cm) | Tumor location | Histologic subtype |
|---|---|---|---|---|
| 1 | 56/M | 10 × 5 × 3 | Neck P | Lymphoma, centrocytic-centroblastic, G II |
| 2 | 61/M | 0, 5 × 1, 5<br>4 × 0, 5 | Eyelids<br>l.a. P | Lymphoma, centrocytic diffuse, G I |
| 3 | 42/F | 2, 5 × 7<br>2 × 2 × 2 | Neck<br>l.a. P | Lymphoma, centroblasticum diffuse, G II |
| 4 | 54/F | 5 × 3 × 3 | Axilla P | Lymphoma, centrocytic diffuse, G II |
| 5 | 62/M | 5 × 4<br>4 × 3 | Axilla<br>l.a. R | Lymphoma, centrocytic-centroblastic follicular, G I |
| 6 | 73/M | 7 × 5<br>5 × 5 | Abdomen R | Lymphoma, immunoblastic, G III |
| 7 | 41/M | 14 × 10 × 5 | Neck R | Lymphoma, lymphoblastic, G III |
| 8 | 58/M | 5 × 4 × 2 | Neck R | Lymphoma, lymphocytic diffuse, G I |
| 9 | 64/M | 4 × 2<br>3 × 2<br>3 × 2, 5 | Neck<br>l.a. P | Lymphoma, lymphocytic diffuse, G I |
| 10 | 75/F | 4 × 4<br>4 × 4<br>4 × 5 | Axilla R<br>Neck R | Lymphoma, immunoblastic, G III |
| 11 | 81/F | 7 × 6 | Neck R | Lymphoma, small lymphocytic diffuse, G I |
| 12 | 53/F | 4 × 4 | Neck P | Lymphoma, small lymphocytic diffuse, G I |
| 13 | 74/F | 5 × 3 | Inguinal region P | Lymphoma, centrocytic-centroblastic, G II |
| 14 | 55/F | 5 × 2, 5 | Inguinal region P | Lymphoma, centrocytic-centroblastic diffuse, G II |

M = male, F = female, P = studied at presentation, R = studied at relapse, G = grade, and l.a. = lesion on both sides.

flow cytometry from deparaffinized tissue sections in 13 patients (*11*). The preparation of a single-cell suspension from paraffin-embedded tissue was done according to a slight modification of the method described by Hedley et al. (*12*). Flow cytometry was done with a FACStar flow cytometer (Becton-Dickinson Immunocytometry Systems, Mountain View, CA) as described elsewhere using a double-analysis method in which all samples are analyzed at least twice (*13*). The interval between the biopsy and PET was 2 mo, except for Cases 6 and 11 which were obtained 6 mo and 12 mo, respectively, before the study. Because the disease had been stable without any treatment, the S-phase value was accepted in the study.

All subjects had a light, protein-poor breakfast before scanning, and a light lunch between $^{11}$C-methionine and FDG studies. Written informed consent was obtained from all patients. The study was approved by the Ethical Committee of Turku University Central Hospital.

## PET Imaging

Carbon-11-methionine and FDG were synthesized at the Turku Medical Cyclotron Laboratory as described elsewhere (*14–16*). The radiochemical purity of $^{11}$C-methionine ranged from 90% to 98%, except in one case (Patient 13), where it was 82%. the radiochemical purity of FDG was over 97%, except in two cases, Patients 6 and 9, where it was 78% and 88%, respectively. The radiochemical impurity consisted of a triacetylated precursor of FDG. The fraction of mannose was 14% with a deviation of 5%.

Transmission scans were recorded for attenuation correction. After transmission scanning, $^{11}$C-methionine (125–300 MBq) was injected into a peripheral vein of the upper extremity. On the same day, FDG (230–340 MBq) was injected intravenously about 4 hr after $^{11}$C-methionine injection. A new transmission scan was performed before the FDG injection. Following the injections, sequential images were recorded for 40 min in the $^{11}$C-methionine studies and for 60 min in the FDG studies using an ECAT Scanner 931/08-12 (*17*). The scanner acquires 15 contiguous slices simultaneously with a slice thickness of 6.7 mm and full width at half maximum is 6.1 mm transaxially in the center of the field of view.

The tumors were positioned by palpation, except for one abdominal lymphoma, where a computed tomographic scan was used.

## Blood Sampling

Frequent venous blood samples were taken from an antecubital vein contralateral to the injection site. The hand and arm were warmed up with a pad thermostated to +40°C. The blood samples were immediately centrifuged, and radioactivity of the plasma was determined. When $^{11}$C-methionine was used as the tracer, the low molecular weight fraction of plasma taken at 10, 20, 40, and 60 min after injection was separated by fast gel

filtration with Sephadex PD-10 columns (Pharmacia Fine Chemicals, Sweden) for radioactivity measurements (*18*).

### Regions of Interest

Regions of interest (ROIs) were selected to represent the tumor area of high accumulation. ROIs were not directly compared to conventional imaging, but clinical radiologic images were used for reference together with palpation. The tumors were of a sufficient size (Table 1). for easy localization and positioning. The minimum number of pixels in a ROI was 43. Relative standard deviation of the ROIs was under 15% in the last frames of the studies. Two or more tumors of four patients were evaluated, but the time-activity curves of different ROIs drawn in the hot spots of the tumors were so similar that we decided to use the average of these curves in analysis.

### Kinetical and Statistical Analysis

A graphical approach according to Patlak et al. and Gjedde (*19,20*) was used to analyze the kinetics of $^{11}$C-methionine and FDG uptake. In this method normalized plasma time values are plotted on the horizontal, and tissue activity values divided by plasma activity values on the vertical axis (Figs. 2–4):

$$x(T) = \int_0^t C_P(t)dt/C_P(T)$$

$$y(T) = C_n(T)/C_p(T),$$

where $C_p(t)$ is plasma concentration of tracer at time t, T is frame mean time after injection, and $C_n(T)$ is tracer concentration of tumor tissue at time T. When y(T) is plotted against x(T) a straight line with a slope of $K_i$ (influx constant) is obtained, which represents the accumulation rate of the tracer in the irreversible compartment.

The influx constant was calculated from the 5–7 last data points in the Patlak curve representing the evaluation time from 15 min till the end of the study (40 min in the $^{11}$C-methionine study and 60 min in the FDG study).

Standardized uptake values (SUV) were also calculated for each patient:

$$SUV = \text{tumor activity}/(\text{dose}/\text{patient's weight}),$$

where tumor activity is the activity measured in the PET study and dose is the injected tracer dose.

The $K_i$-values and SUVs could not be calculated for Patient 2 because the tumors were not visible in the PET images and a reference study could not be done because of the patient's poor condition. The $^{11}$C-methionine uptake in Patient 5 and the FDG uptake in Patient 10 could not be studied because of technical problems.

The $K_i$ of $^{11}$C-methionine and FDG were compared by Wilcoxon's rank sum test for unpaired data (Mann-Whitney's test). $K_i$-values and S-phase fractions were compared by calculating Pearson's correlation coefficient and by cluster-analysis. P values are two-tailed.

## RESULTS

Carbon-11-methionine accumulated in all but one of the lymphomas (Table 2). The patient without clear uptake (Patient 2) had intermediate-grade lymphoma with tumors $0.5 \times 1.5$ and $4 \times 0.5$ cm in diameter in both upper eyelids, and the high accumulation of $^{11}$C-methionine in the lacrimal glands may have impaired the detection of lymphoma in this case.

FDG accumulated in all high-grade lymphomas (n = 3). In two of the five intermediate-grade and three of the five low-grade malignant lymphomas, FDG uptake rate was low ($K_i < 0.02$, Table 2). Since the accumulation and pharmacokinetics of FDG in Patients 6 and 9 who were studied with a batch of FDG containing triacetylglucal were in agreement with that found in the other patients, these results were considered valid and included in the study.

The uptake rate of $^{11}$C-methionine in lymphoma was

**TABLE 2**
Uptake of $^{11}$C-Methionine and FDG by Non-Hodgkin's Lymphoma

| Patient no. | Histologic grade | S-phase | % Uptake rate ($K_i$) | | SUV | |
|---|---|---|---|---|---|---|
| | | | Methionine | FDG | Met | FDG |
| 1 | II | 8.1 | 0.0987 | 0.0415 | 5.7 | 9.1 |
| 2 | II | 4.3 | n | n | n | n |
| 3 | II | 10.9 | 0.0499 | 0.0145 | 4.5 | 3.2 |
| 4 | II | 5.6 | 0.0724 | 0.0293 | 8.4 | 7.7 |
| 5 | I | 7.5 | nd | 0.0470 | nd | 11.0 |
| 6 | III | 13.4 | 0.1027 | 0.0859 | 9.1 | 19.4 |
| 7 | III | 20.0 | 0.1033 | 0.0269 | 5.9 | 8.8 |
| 8 | I | nd | 0.0645 | 0.0098 | 3.9 | 1.9 |
| 9 | I | 3.6 | 0.0537 | 0.0131 | 5.5 | 3.7 |
| 10 | III | nd | 0.1026 | nd | 7.6 | nd |
| 11 | I | 10.3 | 0.0357* | 0.0091 | 3.9 | 2.3 |
| 12 | I | 5.6 | 0.0894 | 0.0218 | 11.7 | 4.7 |
| 13 | III | 11.4 | 0.0812 | 0.1047 | 9.6 | 13.8 |
| 14 | II | 5.9 | 0.0336 | 0.0221 | 2.3 | 4.5 |

* Total plasma activity is used as the input function.
n = No clear accumulation, the $K_i$ value was not calculated, see text.
nd = Not determined.

higher than that of FDG ($p < 0.01$, Table 2). The average uptake rate of $^{11}$C-methionine was 0.0775 ± 0.0245 (s.d.) $min^{-1}$ and of FDG 0.0355 ± 0.0293 $min^{-1}$. The average SUV for $^{11}$C-methionine was 6.7 ± 2.8 and for FDG 7.5 ± 5.3 (Table 2).

Accumulation of both tracers was generally homogeneous, but two high-grade lymphomas (Cases 6 and 7, Table 1, Fig. 1) had clearly heterogeneous uptake of both tracers with areas of very low uptake. The areas of low tracer activity, probably caused by tumor necrosis (Fig. 1), were disregarded when tracer accumulation was assessed.

More than one tumor of Patients 3, 6, 9, and 10 (Table 1) were imaged. The time-activity curves of the different tumors in the individual patients were very similar (Fig. 2) and were regarded to be caused by the disease of the same kind. The average of these time-activity curves was included in the analysis.

The proportion of radioactivity in the low molecular weight fraction of the plasma was 79% ± 9% (s.d.) at 30 min, 67% ± 12% at 40 min, and 48% ± 15% at 60 min after injection of $^{11}$C-methionine (Table 3). When the low molecular weight fraction of plasma radioactivity was used as the input function, the curve $C_n(T)/C_p(T)$ versus plasma time in the Patlak analysis became linear, which indicates that there is net influx of the tracer into the cells.

The tumor/plasma ratio $C_n(T)/C_p(T)$ of both $^{11}$C-methionine and FDG increased faster in high- and intermediate-grade lymphomas when compared to low-grade lymphomas (Figs. 3–4). There was, however, considerable overlap between the histologic grades (Fig. 5).

The uptake rate of $^{11}$C-methionine tended to be higher in lymphomas with a large S-phase fraction ($r = 0.62$, $n = 9$). The uptake rate of FDG correlated poorly with the size of the S-phase fraction ($r = 0.29$, $n = 11$), because in three cases the measured S% was clearly higher than expected from FDG accumulation (Figs. 6–7). The SUV of $^{11}$C-methionine did not correlate at all with S-phase fraction ($r = -0.0052$, $n = 9$). The correlation coefficient was 0.40 (r, $n = 11$) for FDG SUV and S-phase. The correlation between $K_i$ and SUVs was quite good, for $^{11}$C-methionine $r = 0.62$ and for FDG $r = 0.91$.

In the FDG study, the high-grade lymphomas (Cases 6 and 13) were one group in cluster analysis (FDG SUV, FDG $K_i$ and S-Phase as factors). When results from both $^{11}$C-methionine and FDG studies were included in the

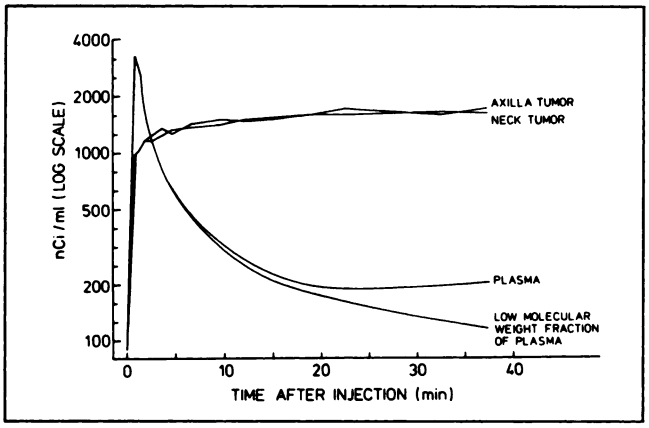


**FIGURE 2.** Time-activity curves of $^{11}$C-methionine study of Patient 10 with both axillary (tumor) and neck tumors (neck tumor) from immunoblastic lymphoma.

**TABLE 3**
Low Molecular Weight Fraction of Total Plasma Activity

| Patient no. | 30 min | 40 min | 60 min |
|---|---|---|---|
| 1 | 0.75 | 0.55 | 0.40 |
| 2 | 0.80 | 0.58 | 0.32 |
| 3 | 0.89 | 0.87 | 0.51 |
| 4 | 0.84 | 0.79 | 0.71 |
| 5 | — | — | — |
| 6 | 0.71 | 0.58 | 0.28 |
| 7 | 0.67 | 0.50 | 0.32 |
| 8 | 0.86 | 0.79 | — |
| 9 | 1.0 | 0.81 | 0.63 |
| 10 | 0.75 | 0.56 | 0.37 |
| 11 | — | — | — |
| 12 | 0.75 | 0.71 | 0.60 |
| 13 | 0.73 | 0.69 | 0.61 |

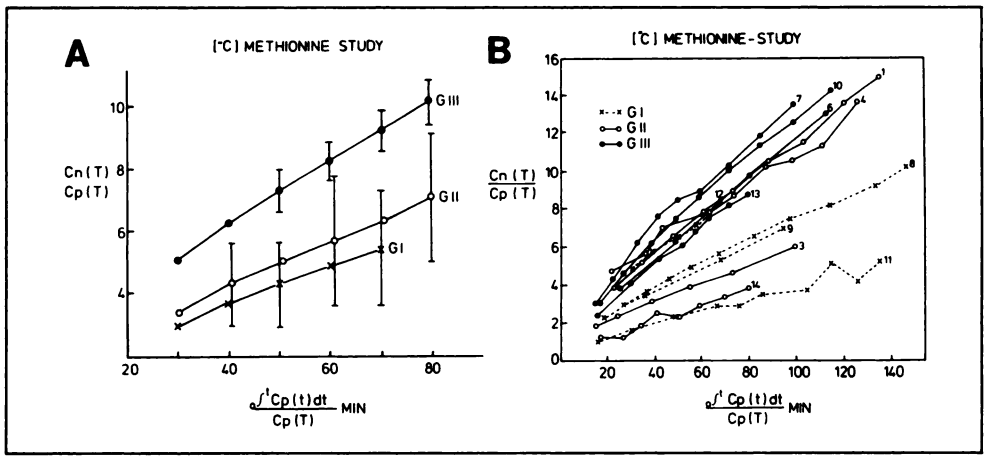


**FIGURE 3.** (A) Average Patlak graphs of $^{11}$C-methionine accumulation rate for low-grade (G I), intermediate-grade (G II), and high-grade (G III) lymphomas. Standard deviation is indicated with bars. Case 2 is excluded. (B) Individual Patlak slopes of $^{11}$C-methionine accumulation. Patient number is in the end of each slope.

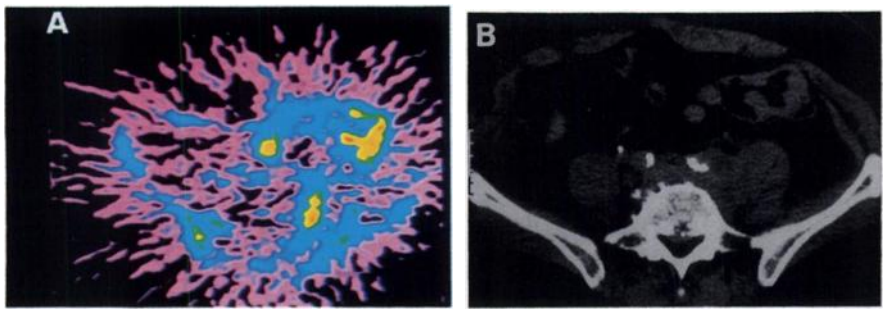


**FIGURE 1.** (A) PET image of Patient 6. Carbon-11-methionine accumulation is clearly seen in the large partially necrotic tumor in the abdomen consisting of immunoblastic lymphoma (high-grade). The necrotic part of the tumor does not accumulate methionine. The image is summed up over 15–40 min postinjection. The injected dose of $^{11}$C-methionine was 260 MBq. Total counts of the image was 7 × $10^5$. (B) CT scan from the same plane.

cluster analysis, Patients 6 and 13 were distinguished as one group. When only $^{11}$C-methionine study was concerned, Patients 6, 7, 12, 13, 1, and 4 were in the same group. In cluster analysis, FDG seems to be better in distinguishing the high-grade tumors from the other lymphoma tumors.

## DISCUSSION

Selenium-75-methionine was reported to accumulate in lymphoma more than 20 yr ago (*21*), but selenate and selenite alone enter lymphoma if administered intravenously (*22*). An increased accumulation of $^{11}$C-methionine and a correlation between histology and $^{11}$C-methionine uptake have been reported for brain and lung tumors (*23–29*). High accumulation of methionine has also been detected in prolactinomas (*30*).

A weak correlation between $^{11}$C-methionine uptake and histology was found in this study. The uptake rate of $^{11}$C-methionine in lymphoma tumor tissue is higher than that of FDG. Carbon-11-methionine is also taken up by the normal pancreas and liver (*31*), salivary glands (*32*), and bone marrow, which impairs its role as a tumor-seeking tracer.

FDG has been found to accumulate in lymphoma in a few cases (*33,34*). In these reports, the uptake of FDG has not, however, been analyzed in terms of lymphoma grading. The present findings suggest that the uptake rate of FDG is more rapid in high-grade lymphomas (Fig. 4), and that low-grade lymphomas may not always become visible in the PET images (Table 2). One out of three high-grade tumors had a very low uptake of FDG (Case 7, Tables 1 and 2, Fig. 5). This tumor was partly necrotic, which may impair the uptake of FDG, and only the average metabolic rate of tumor cells is assessed in PET studies, although the hot spots are under observation.

The rate of FDG uptake studied by PET has been reported to correlate with tumor grade (*35,36*) and survival (*37–39*) in patients with brain tumors, although these findings have been criticized (*40*). The rate of FDG uptake into lung tumor tissue is increased in comparison with normal lung tissue, but there appears to be little correlation between the tumor type and the rate of FDG uptake (*41*). There is also increased accumulation of FDG in colorectal tumors (*42,43*), breast cancer (*44*), head and neck tumors (*45*), thyroid cancer (*46*), and in abdominal abscesses (*47*).

Arterial samples should be taken, if entirely correct information about input function is needed (*48*). Venous samples taken from a heated hand vein can, however, approximate the arterial measurements (*49*).

Standardizing the tumor uptake to blood activity has the advantage of permitting the comparison of uptake kinetics of different tracers, while SUVs cannot be compared between two tracers because of the different biodistribution of the tracers.

The low molecular weight fraction of plasma does not consist only of $^{11}$C-methionine but also of other active

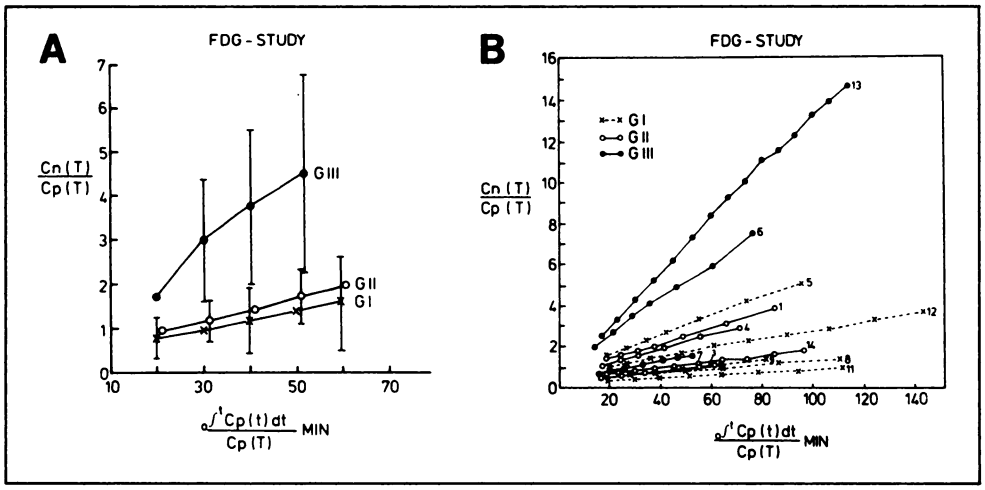


**FIGURE 4.** (A) Average Patlak graphs of FDG accumulation rate for low-grade (G I), intermediate-grade (G II), and high-grade (G III) lymphomas. Standard deviation is indicated with bars. (B) Individual Patlak slopes of FDG accumulation. Patient number is in the end of each slope.

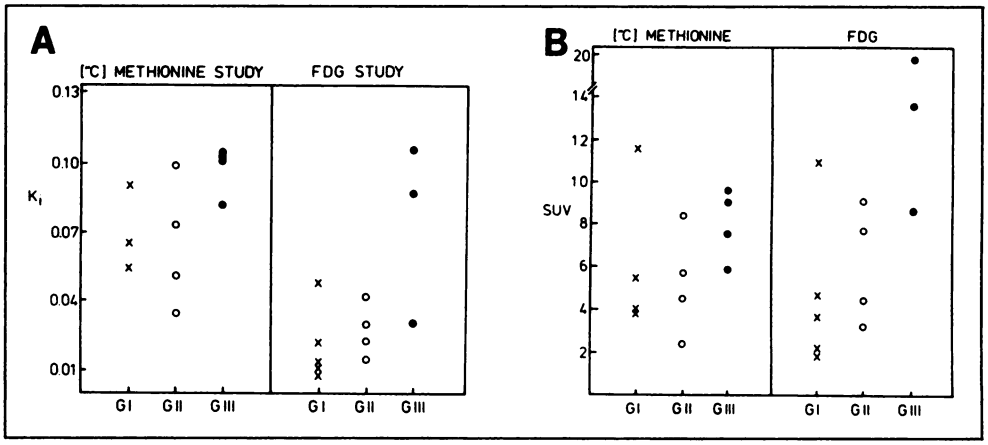


**FIGURE 5.** (A) $K_i$-values of $^{11}$C-methionine and FDG in non-Hodgkin's lymphoma according to histologic grade. Results from Patient 2 with uncertain accumulation due to proximity of the larcimal glands are not shown, and the $K_i$-value of $^{11}$C-methionine accumulation rate of Patient 11 where only total plasma was available is not included. (B) SUVs of $^{11}$C-methionine and FDG studies.

light molecules, such as serine (*18*). The fraction of protein free $^{11}$C-labeled methionine of the total plasma radioactivity measured with high-pressure liquid chromatography has been reported to be about 71% at 30 min after injection and about 36% at 60 min postinjection (*50*), values which are about 10% smaller than the ones we obtained by the fast gel filtration method. Serine is not transported across the blood-brain barrier as fast as methionine (*51*), but the transport system in cancer cell plasma membrane is nonspecific and the uptake of serine may be of significance.

The graphical analysis method of Patlak et al. (*19*) is an established method to assess the rate of FDG uptake. This method formerly has been applied to $^{11}$C-methionine (*52, 53*). Although the kinetics of $^{11}$C-methionine transport through plasma membranes is not the same as that of FDG, there was a net influx of the tracer into the tumor and the method appears to be of value in $^{11}$C-methionine study.

The local blood flow and blood volume may vary in different tumors and affect the accumulation of tracers. The mean blood flow in human lymphomas has been reported to be 35 ± 21 ml/min/100 g, which is higher than for carcinomas (*54*). There is also no significant correlation between the size of the tumor and the local blood flow.

NHL is a disease of heterogeneous clinical presentation. Low-grade malignant lymphomas have a prolonged clinical course, typically of several years, whereas high-grade malignant lymphomas may be fatal within a few weeks. Both histology and the size of S-phase fraction are associated with survival in NHL. However, there are difficulties in the determination of histology, such as interobserver variability (*55*). Proliferation by cytometry is, on the other hand, disturbed by cell debris and a lack of knowledge about cell cycle time (*56*).

The membrane transport systems used in the uptake of nutrients (e.g., of sugars and amino acids) is frequently enhanced in transformed cells. Similar changes may occur during increased cell proliferation stimulated by, for example, growth factors or mitogens (*57*). Although only secondarily related to the malignant phenotype, the rates of glucose and amino acid metabolism are probably closely related to the proliferation rate of lymphoma. Tumors may, however, be heterogeneous not only macroscopically

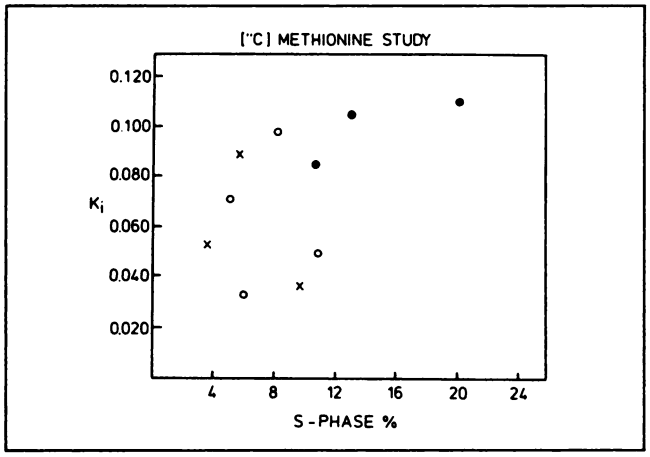


**FIGURE 6.** Correlation of $K_i$-values of $^{11}$C-methionine uptake and S-phase fractions in nine patients with non-Hodgkin's lymphoma, r = 0.62. Symbols as in Figure 3.

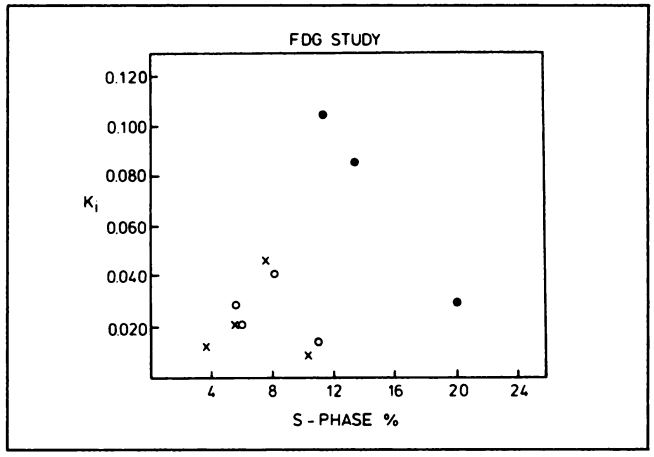


**FIGURE 7.** Correlation of $K_i$-values of FDG uptake and S-phase fraction in 11 patients with non-Hodgkin's lymphoma, r = 0.29. Symbols are as defined in Figure 3.

(our Cases 6 and 7), but also at a microscopic and at a metabolic level, in which cases only the average metabolic activity will be measured by PET. PET and FDG may serve as an alternative to assess tumor grades, especially when there is uncertainty about the histologic grade.

## ACKNOWLEDGMENTS

The authors acknowledge the support of Professor Eeva Nordman and Professor Uno Wegelius, and thank Dr. Heikki Minn, Dr. Aapo Ahonen, and Dr. Robert Paul for fruitful discussions, Dr. Karl-Ove Söderström for reexamination of the histologic tumor samples, Merja Haaparanta-Solin, MSc and the Turku Medical Cyclotron Laboratory for providing the FDG, as well as the personnel of the nuclear medicine department for accurate work in collecting the data.

The study was financially supported by grants from the Finnish Cancer Society and the Arvo and Inkeri Suominen Foundation.

## REFERENCES

1. Gallagher BM, Fowler JS, Gutterson NI, et al. Metabolic trapping as a principle of radiopharmaceutical design: some factors responsible for the biodistribution of [$^{18}$F]2-deoxy-2-fluoro-D-glucose. *J Nucl Med* 1978; 19:1154–1161.
2. Sols A, Crane RK. Substrate specificity of brain hexokinase. *J Biol Chem* 1954;210:581–595.
3. Bessell EM, Thomas P. The effect of substitution at C-2 of D-glucose 6-phosphate on the rate of dehydrogenation by glucose-6-phosphate dehydrogenase (from yeast and from rat liver). *Biochem J* 1973;131:83–89.
4. Weber G. Enzymology of cancer cells (second of two parts). *New Engl J Med* 1977;296:541–551.
5. Hoffman RM. Altered methionine metabolism, DNA methylation and oncogenic expression in carcinogenesis. *Biochem Biophys Acta* 1984; 738:49–87.
6. Stern PH, Wallace CD, Hoffman RM. Altered methionine metabolism occurs in all members of a set of diverse human tumor cell lines. *J Cell Physiol* 1984;119:29–34.
7. Wheatley DN. On the problem of linear incorporation of amino acids into cell proteins. *Experientia* 1982;38:818–820.
8. Stern PH, Hoffman RM. Elevated overall rates of transmethylation in cell lines from diverse human tumors. *In Vitro* 1984;20:663–670.
9. Isselbacher KJ. Increased uptake of amino acids and 2-deoxy-D-glucose by virus-transformed cells in culture. *Proc Nat Acad Sci USA* 1972;69:585–589.
10. The non-Hodgkin's Lymphoma Pathologic Classification Project. National Cancer Institute sponsored study of classifications of non-Hodgkin's lymphomas. Summary and description of a Working Formulation for clinical usage. *Cancer* 1982;49:2112–2135.
11. Joensuu H, Klemi PJ, Korkeila E. Prognostic value of DNA ploidy and proliferative activity in Hodgkin's disease. *Am J Clin Pathol* 1988;90:670–673.
12. Hedley DW, Friedlander ML, Taylor IW, Rugg CA, Musgrove EA. Method for analysis of cellular DNA content of paraffin-embedded pathological material using flow cytometry. *J Histochem Cytochem* 1983;31:1333–1335.
13. Joensuu H, Klemi PJ. DNA aneuploidy in adenomas of the endocrine organs. *Am J Pathol* 1988;132:145–151.
14. Långström B, Antoni G, Gullberg P, et al. Synthesis of L- and D-[methyl-$^{11}$C]methionine. *J Nucl Med* 1987;28:1037–1040.
15. Någren K, Aho K, Bergman J, et al. $^{11}$C-methyl iodide: routine production and use in preparation of some $^{11}$C-labelled radiopharmaceuticals for PET in Turku. In: Brenner M, Bergman J, Brenner R, Lill J-O, Manngård P, eds. *The Åbo Akademi accelator laboratory triennal report 1987–1989.* Turku, 1990:76–81.
16. Haaparanta M, Bergman J, Solin O, et al. A remotely controlled system for the routine synthesis of $^{18}$F-2-fluoro-2-deoxy-D-glucose. *Nuclearmedizin* 1984;21(suppl):823–826.
17. Spinks TJ, Jones T, Gilardi MC, Heather JD. Physical performance of the latest generation of commercial positron scanner. *IEEE Trans Nucl Sci* 1988;35:721–725.
18. Lundqvist H, Stålnacke C-G, Långström B, Jones B. Labelled metabolites in plasma after i.v. administration of [$^{11}$Ch$_3$]-L-methionine. In: Greits T, Widen L, Ingvar D, eds. *The metabolism of the human brain studied with positron emission tomography.* New York: Raven Press; 1985:233–240.
19. Patlak CS, Blasberg RG, Fenstermacher JD. Graphical evaluation of blood-to-brain transfer constants from multiple-time uptake data. *J Cereb Blood Flow Metab* 1983;3:1–7.
20. Gjedde A. High- and low-affinity transport of D-glucose from blood to brain. *J Neurochem* 1981;36:1463–1471.
21. Herrera NE, Gonzalez R, Schwartz RD, Diggs AM, Belsky J. Se-75-methionine as a diagnostic agent in malignant lymphoma. *J Nucl Med* 1965;6:792–804.
22. Spencer RP, Montana G, Scanlon GT, Evans OR. Uptake of selenomethionine by mouse and human lymphomas, with observations on selenite and selenate. *J Nucl Med* 1967;8:197–208.
23. Bustany P, Chatel M, Derlon JM, et al. Brain tumor protein synthesis and histological grades: a study by positron emission tomography (PET) and C-11-L-methionine. *J Neurooncol* 1986;3:397–404.
24. Schober O, Meyer G-J, Duden C, et al. Die Aufnahme von Aminosäuren in Hirntumoren mit der Positronen-Emissionstomographie als Indikator für die Beurteilung von Stoffwechselaktivität und Malignität. *Fortschr Röntgenstr* 1987;147:503–509.
25. Mosskin M, von Holst H, Bergström M, et al. Positron emission tomography with $^{11}$C-methionine and computed tomography of intracranial tumours compared with histopathologic examination of multiple biopsies. *Acta Radiol* 1987;28:673–681.
26. Ericson K, Lilja A, Bergström M, et al. Positron emission tomography with ([$^{11}$C]methyl)-L-methionine, ([$^{11}$C]-D-glucose, and [$^{68}$Ga]EDTA in supratentorial tumors. *J Comput Assist Tomogr* 1985;9:683–689.
27. Bergström M, Collins VP, Ehrin E, et al. Discrepancies in brain tumor extent as shown by computed tomography and positron emission tomography using [$^{68}$Ga]EDTA, [$^{11}$C]Glucose, and [$^{11}$C]methionine. *J Comput Assist Tomogr* 1983;7:1062–1066.
28. Fujiwara T, Matsuzawa T, Kubota K, et al. Relationship between histologic type of primary lung cancer and carbon-11-L-methionine uptake with positron emission tomography. *J Nucl Med* 1989;30:33–37.
29. Kubota K, Matsuzawa T, Ito M, et al. Lung tumor imaging by positron emission tomography using C-11-L-methionine. *J Nucl Med* 1985;26:37–42.
30. Bergström M, Muhr C, Lundberg PO, et al. In vivo study of amino acid distribution and metabolism in pituitary adenomas using positron emission tomography with D-$^{11}$C-methionine and L-$^{11}$C-methionine. *J Comput Assist Tomogr* 1987;11:384–389.
31. Syrota A, Duquesnoy N, Paraf A, Kellershohn C. The role of positron emission tomography in the detection of pancreatic disease. *Radiology* 1982;143:249–253.
32. Syrota A, Collard P, Paraf A. Comparison of $^{11}$C-L-methionine uptake by the parotid gland and pancreas in chronic pancreatitis studied by positron emission tomography. *Gut* 1983;24:637–641.
33. Paul R. Comparison of fluorine-18-2-fluorodeoxyglucose and gallium-67-citrate imaging for detection of lymphoma. *J Nucl Med* 1987;28:288–92.
34. Kuwabara Y, Ichiya Y, Otsuka M, et al. High [$^{18}$F]FDG uptake in primary cerebral lymphoma: a PET study. *J Comput Assist Tomogr* 1988;12:47–48.
35. DiChiro G, DeLaPaz RL, Brooks RA, et al. Glucose utilization of cerebral gliomas measured by [$^{18}$F]fluorodeoxyglucose and positron emission tomography. *Neurology* 1982;32:1323–1329.
36. DiChiro G. Positron emission tomography using [$^{18}$F]fluorodeoxyglucose in brain tumors—a powerful diagnostic and prognostic tool. *Invest Radiol* 1986;22:360–371.
37. Patronas NJ, DiChiro G, Kufta C, et al. Prediction of survival in glioma patients by means of positron emission tomography. *J Neurosurg* 1985;62:816–822.
38. Alavi JB, Alavi A, Chawluk J, et al. Positron emission tomography in patients with glioma—a predictor of prognosis. *Cancer* 1988;62:1074–1078.
39. DiChiro G, Hatazawa J, Katz DA, Rizzoli HV, De Michele DJ. Glucose utilization by intracranial meningeomas as an index of tumor aggressivity and probability of recurrence: a PET study. *Radiology* 1987;164:521–526.
40. Tyler JL, Diksic M, Villemure J-G, et al. Metabolic and hemodynamic evaluation of gliomas using positron emission tomography. *J Nucl Med* 1987;28:1123–1133.
41. Nolop KB, Rhodes CG, Brudin LH, et al. Glucose utilization in vivo by human pulmonary neoplasms. *Cancer* 1987;60:2682–2689.
42. Yonekura, Y, Benua RS, Brill AB, et al. Increased accumulation of 2-deoxy-2-[$^{18}$F]fluoro-D-glucose in liver metastases from colon carcinoma. *J*

*Nucl Med* 1982;23:1133–1137.
43. Strauss LG, Clorius JH, Schlag P, et al. Recurrence of colorectal tumors: PET evaluation. *Radiology* 1989;170:329–332.
44. Minn H, Soini I. [$^{18}$F]Fluorodeoxyglucose scintigraphy in diagnosis and follow-up of treatment in advanced breast cancer. *Eur J Nucl Med* 1989;15:61–66
45. Minn H, Joensuu H, Ahonen A, Klemi P. Fluorodeoxyglucose imaging: a method to assess the proliferative activity of human cancer in vivo. Comparison with DNA flow cytometry in head and neck tumors. *Cancer* 1988;61:1776–1781.
46. Joensuu H, Ahonen A. Imaging of metastases of thyroid carcinoma with fluorine-18-fluorodeoxyglucose. *J Nucl Med* 1987;28:910–914.
47. Tahara T, Ichiya Y, Kuwabara Y, et al. High [$^{18}$F]fluorodeoxyglucose uptake in abdominal abscesses: a PET study. *J Comput Assist Tomogr* 1989;13:829–831.
48. Green JH, Ellis FR, Shallcross TM, Bramley PN. Invalidity of hand heating as a method to arterialize venous blood. *Clin Chem* 1990;36:719–722.
49. Abumrad NN, Rabin D, Diamond MP, Lacy WW. Use of a heated superficial hand vein as an alternative site for the measurement of amino acid concentration and for the study of glucose and alanine kinetics in man. *Metabolism* 1981;30:936–940.
50. Ishiwata K, Hatazawa J, Kubota K, et al. Metabolic fate of L-[methyl-$^{11}$C] methionine in human plasma. *Eur J Nucl Med* 1989;15:665–669.
51. Oldendorf WH. Brain uptake of radiolabeled amino acids, amines and hexoses after arterial injection. *Am J Physiol* 1971;221:1629–1639.
52. Hatazawa J, Ishiwata K, Itoh M, et al. Quantitative evaluation of L-[methyl-C-11]methionine uptake in tumor using positron emission tomography. *J Nucl Med* 1989;30:1809–1813.
53. Bergström M, Muhr C, Lundberg PO, Bergström K, Lundqvist H, Långström B. Amino acid metabolism in pituitary adenomas. *Acta Radiol* 1986;26(suppl 369):412–414.
54. Mäntylä MJ. Regional blood flow in human tumors. *Cancer Res* 1979;39:2304–2306.
55. De Wolf-Peeters C, Caillou B, Diebold J, et al. Reproducibility and prognostic value of different non-Hodgkin's lymphoma classifications: study based on the clinicopathologic relations found in the EORTC trial (20751). *Eur J Cancer Clin Oncol* 1985;21:579–584.
56. Jalkanen S, Joensuu H, Klemi PJ. Prognostic value of lymphocyte homing receptor and S-phase fraction in non-Hodgkin's lymphoma. *Blood* 1991:1549–1556.
57. Ruddon RW. *Cancer biology*, second edition. New York, Oxford: Oxford University Press; 1987:216.

*(continued from page 5A)*

# FIRST IMPRESSIONS

**ACQUISITION INFORMATION:**
A 66-yr-old male was admitted for resection of a right atrial mass. A ventilation-perfusion scan was performed preoperatively to evaluate progressive hypoxemia. The perfusion phase demonstrates myocardial uptake of $^{99m}$Tc-MAA, indicating a right-to-left shunt made apparent by a large photopenic area surrounding the heart. An echocardiogram demonstrated a solid mass occupying the right atrium and a pericardial effusion, non-Hodgkin's lymphoma with invasion of the atrial septum was found at surgery.

**TRACER:**
Technetium-99m-MAA

**ROUTE OF ADMINISTRATION:**
Intravenous

**INSTRUMENTATION:**
ADAC Genesys Camera

**CONTRIBUTORS:**
W.H. McCuskey, MD and E. Turbiner, DO

**INSTITUTION:**
Mercy Hospital of Pittsburgh, Pittsburgh, PA